Structure/Property Correlations in Ion-Conducting Mixed-Network Former Glasses: Solid-State NMR Studies of the System $Na_2O-B_2O_3-P_2O_5$

Dominika Zielniok,† Cornelia Cramer, and Hellmut Eckert*

Institut für Physikalische Chemie and Sonderforschungsbereich 458, Westfälische Wilhelms-Universität Münster, Corrensstrasse 30/36, D-48149 Münster, Germany

Received November 24, 2006. Revised Manuscript Received April 6, 2007

The structural organization of sodium borophosphate glasses with composition $(Na_2O)_{0.4}[(B_2O_3)_x(P_2O_5)_{1-x}]_{0.6}$ ($0.0 \leq x \leq 1.0$) has been investigated by ^{11}B and ^{31}P magic-angle spinnning (MAS) NMR spectroscopy. Spectral deconvolutions and established chemical shift trends yield a detailed quantitative account of the local structural units present in these glasses. These units can be described in terms of coordination polyhedra $P^{(n)}_{mB}$ and $B^{(n)}_{mP}$, where n reflects the number of bridging oxygen atoms and mB $\leq n$ and mP $\leq n$ are the number of connected boron and phosphorus species, respectively. The favorable interaction between the two network formers boron oxide and phosphorus oxide results in the dominant formation of B−O−P linkages. Compared to binary sodium phosphate and borate glasses, the extent of network polymerization is significantly increased, particularly within the region $0 \leq x \leq 0.4$, caused by the preferential formation of four-coordinate boron species linked to phosphorus. Glasses with higher boron contents also contain three-coordinated $BO_{3/2}$ units, which appear to interact only weakly with phosphorus. The NMR spectra can be analyzed in terms of the concentration of bridging oxygen atoms per network former species, [O], and divided into the quantitative contributions from P−O−P, P−O−B, and B−O−B linkages. [O] reveals a nonlinear compositional trend showing an excellent correlation with macroscopic properties such as glass-transition temperatures, densities, and ionic-conductivity parameters.

Introduction

Ion-conducting glasses are an important class of solid electrolytes that have already experienced widespread application in energy-storage devices. For the development of higher-performance materials a fundamental understanding of the phenomenon of ion transport in glasses is essential.[1] To this end, a large amount of structural information has been obtained concerning the local environments of the cations and their spatial distribution in binary alkali borate, silicate, and phosphate glasses.[2−5] The structures of such glasses are based on two- or three-dimensional networks created by the main group oxide (network former species). By addition of alkaline oxides (the so-called network-modifier species), anionic sites are generated in this network, which compensate the positive charge of the mobile cations. The electrical dc conductivities are simply given by the product of ionic charge, ionic mobility, and mobile ion concentration. When considering the compositional dependence of ion conductivities in glassy electrolytes, it is important to keep in mind, however, that ionic mobilities themselves are intrinsically concentration dependent,[6] as they result from a complex interplay of structural parameters, which are affected by the glass composition and hence the ion content of the glass. These factors include (a) the depth of the potential well characterizing the cation−anion Coulombic attractions, (b) the strain imposed by ionic motion upon the network, (c) the average jump distance for the ions to be overcome, and (d) the number of well-matched target sites in the vicinity of the mobile ions. In an effort of developing a fundamental understanding of the structure/function relationships, researchers have systematically studied the effect of ion concentration on modifier content for a number of binary alkaline-containing oxide glasses.[7] For each of these binary systems, the experimentally found increase in ionic conductivity with increasing network-modifier content is not unexpected because these parameters are generally influenced by higher cation contents in a favorable way: average jump distances become shorter, the number of potential target sites increases, and in many cases, glasses containing higher alkaline ion concentrations feature a less strongly polymerized network, which tends to diminish the mechanical strain effect. To understand the effect of each of the control parameters a−d it would thus be of great interest to study the influence of local structure on cation mobility along compositional lines with approximately

* Corresponding author. E-mail: eckerth@uni-muenster.de.
† Present address: Fachbereich Chemie der Philipps−Universität Marburg, Hans-Meerwein-Strasse, D-35043 Marburg, Germany.

(1) Magistris, A. In *Fast Ion Transport in Glasses*; Scrosati, S., Ed.; Klüwer: Dordrecht, The Netherlands, 1992; p 213 and references therein.
(2) Velli, L. L.; Varsamis, C. P. E.; Kamitsos, E. I.; Moncke, D.; Ehrt, D. *Phys. Chem. Glasses* **2005**, *46* (2), 178.
(3) Kamitsos, E. I. *Phys. Chem. Glasses* **2003**, *44*, 79.
(4) Ratai, E.; Chan, J. C. C.; Eckert, H. *Phys. Chem. Chem. Phys.* **2002**, *4*, 3198.
(5) Eckert, H.; Elbers, S.; Epping, J. D.; Janssen, M.; Kalwei, M.; Strojek, W.; Voigt, U. *Top. Curr. Chem.* **2004**, *246*, 195.
(6) Bunde, A.; Ingram, M. D.; Maass, P. *J. Non-Cryst. Solids* **1994**, *172-174*, 1222.
(7) Bunde, A. *Solid State Ionics* **1998**, *105*, 1.

10.1021/cm0628092 CCC: $37.00
Published on Web 06/01/2007

Table 1. Boron Oxide Content x of Glassy $(Na_2O)_{0.4}[(B_2O_3)_x[P_2O_5)_{1-x})]_{0.6}$, Densities ρ, Molar Volumes V_M, Sodium Ion Number Densities N_V, Glass-Transition Temperatures T_g, Logarithms of the Electrical dc Conductivities σ_{dc} at 298 K, and Activation Energies E_a of $\sigma_{dc}T$ in the Glasses under Study

x	ρ (g/cm^3) (± 0.3%)	V_M (cm^3 mol^{-1}) (± 0.3%)	N_V (× 10^{22} cm^{-3}) (± 0.3%)	T_g (K) (± 2 K)	log(σ_{dc} @ 298 K) ((Ω cm)$^{-1}$) (± 1%)	E_a (eV) (± 0.02)
0	2.47	44.36	1.09	535	−11.298	0.90
0.1	2.48	42.59	1.13	565	−10.941	0.84
0.2	2.51	40.35	1.19	620	n.a.	n.a.
0.3	2.52	38.47	1.25	678	−9.250	0.72
0.4	2.56	36.17	1.33	683	−9.054	0.64
0.5	2.55	34.61	1.39	703	−9.012	0.68
0.6	2.51	33.43	1.44	697	−8.978	0.68
0.7	2.49	31.96	1.51	698	−8.875	0.67
0.8	2.45	30.72	1.57	723	−8.630	0.65
0.9	2.43	28.91	1.67	720	−8.600	0.64
1.0	2.39	27.85	1.73	633	−9.110	0.69

constant ion concentrations. Multiple network former systems afford this opportunity. In particular, alkali borophosphate glasses are well-suited for this research objective, as previous results have shown that the successive replacement of the network former species phosphorus oxide by boron oxide at constant alkali content can have a significant influence on the glass transition temperatures and lead to profound structural changes in the network (mixed-network former effect).[8−12] Furthermore, previous NMR studies of binary alkali borate[13] and alkali phosphate glasses[14] have shown that the alkali ions are essentially statistically distributed, thereby avoiding complicating influences of cation segregation and clustering effects on ionic conductivity. With this objective in mind, we have chosen the ternary glass system $(Na_2O)_{0.4}[(B_2O_3)_x(P_2O_5)_{1-x}]_{0.6}$ for a detailed study of composition-dependent ion conductivities and their correlation with local structure. The latter information has been extracted from complementary multinuclear solid-state NMR and Raman spectroscopic experiments. Although the ability of solid-state NMR to provide structural information in alkali borophosphate glasses is well-documented,[15−20] significant progress has been achieved in recent years by the application of advanced dipolar NMR techniques combined with the benefits of high magnetic field strengths and fast magic-angle spinning. This has resulted in quantitative insights about species concentrations and interatomic connectivities to unprecedented detail,[21,22] making solid-state NMR the technique of choice in addressing detailed structure/property correlations. The focus of the present study is the "mixed-network former effect", a pronounced nonlinear dependence of a variety of macroscopic properties (glass-transition temperatures, densities, and ionic conductivities) on the framework composition in the sodium borophosphate glass system $(Na_2O)_{0.4}[(B_2O_3)_x(P_2O_5)_{1-x}]_{0.6}$ ($0.0 \leq x \leq 1.0$). A structural rationale for these effects will be sought on the basis of combined Raman as well as ^{11}B and ^{31}P solid-state NMR spectroscopies.

Experimental Section

Sample Preparation. The sets of glass samples of the ternary system $Na_2O-P_2O_5-B_2O_3$ have been synthesized by traditional melt-cooling methods. Glasses with compositions specified by the general formula: $(Na_2O)_{0.4}[(B_2O_3)_x(P_2O_5)_{1-x}]_{0.6}$ with $0.0 \leq x \leq 1.0$ were prepared as follows: Sodium carbonate (Merck 99.9%), ammonium dihydrogen phosphate (Fluka 99.5%), and diboron trioxide (Merck, 99.95%) were used as starting materials. To obtain water-free reagents,we kept Na_2CO_3 and B_2O_3 at 393 K for more than 48 h in an oven. The weighed chemicals were ground and mixed thoroughly in their desired proportions. Glasses with a high concentration of phosphorus oxide (above 45%) were melted in an alumina crucible, whereas for the other glasses, a platinum crucible was used. In a first step, the mixture of starting materials was preheated inside an electric oven at a temperature of 493 K for 3 h until the decomposition of the starting materials was complete. In the second step, the preheated materials were melted in a closed crucible at 1123 to 1173 K for about 1 h. The homogeneous melts were quenched into preheated sample holders kept at temperatures 20−30 K below T_g. Depending on the glass-forming ability and moisture sensitivity of the samples, stainless steel moulds with different inner diameters were used. The quenched glass samples were annealed about 30 K below their respective glass-transition temperatures for 2.5 h and then cooled from the annealing temperature to room temperature with a controlled cooling rate of 0.5 K/min. Because of the hygroscopic character of the borophosphate glasses, all samples were kept in plastic containers with desiccant.

For impedance measurements, thin cylindrical specimens with a diameter between 16 mm and 28 mm were drilled from glass plates. The cylindrical samples were then cut into slices of approximately 1 to 2 mm thickness using a Struers Accutom-5 machine. After that, all samples were polished with a polishing

(8) Branda, F.; Constantini, A.; Fresa, R.; Buri, A. *Phys. Chem. Glasses* **1995**, *36*, 272.
(9) Constantini, A.; Buri, A.; Branda, F. *Solid State Ionics* **1994**, *67*, 175.
(10) Takebe, H.; Harada, T.; Kuwatara, M. J. *Non-Cryst. Solids* **2006**, *352*, 709. Ahoussou, A. P.; Rogez, J.; Kone, A. *Thermochim. Acta* **2006**, *441*, 96.
(11) Videau, J. J.; Ducel, J. F.; Suh, K. S.; Senegas, J. J. *Alloys Compd.* **1992**, *188*, 157. Ducel, J. F.; Videau, J. *J. Mater Lett.* **1992**, *13*, 271.
(12) Kumar, S.; Vinatier, P.; Levasseur, A.; Rao, K. J. *J. Solid State Chem.* **2004**, *177*, 1723. Anantha, P. S.; Hariharan, K. *Mater. Chem. Phys.* **2005**, *89*, 428.
(13) Epping, J. D.; Strojek, W.; Eckert, H. *Phys. Chem. Chem. Phys.* **2005**, *7*, 2384.
(14) Strojek, W.; Eckert, H. *Phys. Chem. Chem. Phys.* **2006**, *8*, 2276.
(15) Beekenkamp, P.; Hardemann, G. E. G. *Verres Refract.* **1966**, *20*, 419.
(16) Yun, Y. H.; Bray, P. J. J. *Non-Cryst. Solids* **1978**, *30*, 45.
(17) Feng, T.; Linzhang, P. J. *Non-Cryst. Solids* **1989**, *112*, 142.
(18) Villa, M.; Scagliotti, M.; Chiodelli, G. J. *Non-Cryst. Solids* **1987**, *94*, 101.
(19) Koudelka, L.; Mosner, P.; Zeyer, M.; Jäger, C. *Phys. Chem. Glasses* **2002**, *43C*, 102.
(20) Koudelka, L.; Mosner, P.; Zeyer, M.; Jäger, C. *J. Non-Cryst. Solids* **2003**.
(21) Zeyer-Düsterer, M.; Montagne, L.; Palavit, G. Jäger, C. *Solid State Nucl. Magn. Reson.* **2005**, *27*, 50. Zeyer, M.; Montagne, L.; Jäger, C. *Glass Sci. Technol.* **2002**, *75*, 186.
(22) Elbers, S.; Strojek, W.; Koudelka, L.; Eckert, H. *Solid State Nucl. Magn. Reson.* **2005**, *27*, 65.

apparatus (Läpp Machine, $\lambda_{LOGITECH}$) using a mixture of Al_2O_3 powder of 9 μm diameter and liquid ethylene glycol in a volume ratio 1:9. To ensure a continuous and stable contact between the glass sample and the electrodes, the polished faces of each prepared glass sample were sputtered for 450 s with silver and afterward with platinum for 300 s.

Characterization. Glass densities were determined according to the Archimedes principle using ethylene glycol used as a standard liquid ($\rho = 1.11$ g/cm^3). Glass-transition temperatures, T_g, were determined as "onset points" from differential scanning calorimetry (DSC), using a NETZSCH DSC-204 instrument, operated with a linear heating ramp of 10 K/min.

Electrical conductivities were determined from impedance measurements using a Novocontrol Alpha-S high-resolution dielectric analyzer with an alpha-S active sample cell and α-Quatro Cryosystem temperature-control apparatus. Frequency-dependent impedance measurements were carried out isothermally in the frequency range between 1×10^{-2} Hz and 6 MHz and at temperatures between 198 and 548 K. From the low-frequency conductivity plateaus, the dc conductivity for each temperature could be determined.

Raman scatting experiments were conducted on a LabRAM HR 800 high-resolution spectrometer, using the 532.18 nm line of a Nd/YAG laser operating at 8.6 mW as the excitation source. The spectra were collected at room temperature for 420 s with a spectral resolution of 1 cm^{-1}. Single-pulse ^{31}P and ^{11}B MAS NMR spectra were obtained on Bruker DSX 400 and DSX 500 spectrometers, respectively, using a 4 mm MAS NMR probe operated at a spinning rate of 12 kHz. ^{31}P spectra were measured at 162.03 MHz, with a 90° pulse of 4.5 μs length and a relaxation delay time ranging from 300 to 400 s. ^{11}B MAS NMR spectra were recorded at 160.46 MHz using a short pulse of 1 μs length and a relaxation delay of 10 s. Experimental lineshapes were deconvoluted using the DMFIT software.[23] Chemical shifts are reported relative to 85% H_3PO_4 and BF_3-Et_2O solution for ^{31}P and ^{11}B, respectively.

Results, Assignments, and Interpretation

Macroscopic Properties. Table 1 summarizes the densities, as well as the molar volumes and the sodium ion number densities, N_V(Na), calculated from these data. The experimentally determined densities of the mixed sodium borophosphate glasses range between 2.48 and 2.56 g/cm^3 and initially show a clear increase with x, yielding a maximum for $x = 0.4$. A decrease to 2.39 g/cm^3 is observed for the final pure sodium borate composition. Overall, these results agree with trends found in the literature for this glass-forming system.[11,12]

Figure 1 shows the compositional dependence of the glass-transition temperature, whereas panels a and b of Figure 2 show the electrical dc conductivity values at 298 K and the activation energies extracted from temperature-dependent measurements. Note that all three quantities show rather analogous compositional dependences: a steep initial increase (decrease in E_a) in the phosphate-rich region ($0 \le x \le 0.4$), rather marginal changes in the $0.4 \le x \le 0.9$ region, and a steep decrease (increase in E_a) when going from the borate-rich ternary glass to the pure sodium borate endmember composition.

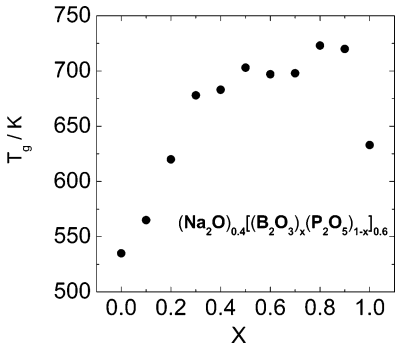

Figure 1. Compositional dependence of the glass-transition temperature T_g in sodium borophosphate glasses in the system $(Na_2O)_{0.4}[(B_2O_3)_x(P_2O_5)_{1-x}]_{0.6}$.

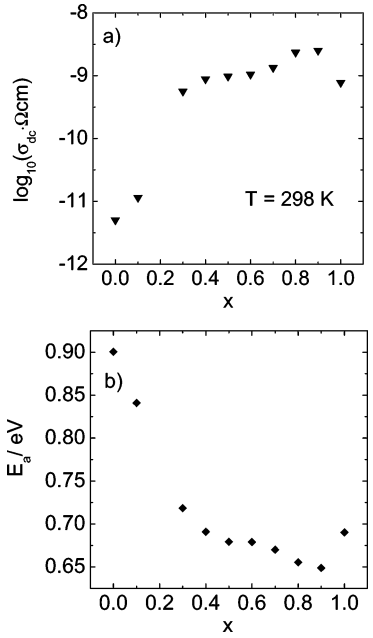

Figure 2. (a) Compositional dependence of the dc electrical conductivity σ_{dc} at 298 K in sodium borophosphate glasses in the system $(Na_2O)_{0.4}[(B_2O_3)_x(P_2O_5)_{1-x}]_{0.6}$. (b) Compositional dependence of the activation energy of $\sigma_{dc}T$ in sodium borophosphate glasses in the system $(Na_2O)_{0.4}[(B_2O_3)_x(P_2O_5)_{1-x}]_{0.6}$.

Raman Spectroscopy. Figure 3 summarizes the Raman spectra. The trends observed in these spectra are in agreement with previously published data on sodium and lithium borophosphate glasses, as well as previous studies of vitreous $NaPO_3$[24,25] and $Na_2B_4O_7$.[26] The Raman spectrum of the binary $(Na_2O)_{0.4}(P_2O_5)_{0.6}$ glass is dominated by two intense lines at 1188 and 1161 cm^{-1}, which are assigned to the asymmetric and symmetric (PO_2) stretching modes, respectively, involving nonbridging oxygen atoms. In addition, a broad band with its intensity maximum at 693 cm^{-1} signifies P−O bond vibrations involving P−O−P bridges. Furthermore, the broad band centered around 1300 cm^{-1} is assigned to the $(P{=}O)_{sym}$ stretching mode originating from the phosphorus in $P^{(3)}$ structural groups. As the boron content is increased, the 1300 cm^{-1} band gradually shifts toward lower frequencies. Fur-

(23) Massiot, D.; Fayon, F.; Capron, M.; King, I.; Le Calve, S.; Alonso, B.; Durand, J. O.; Bujoli, B.; Gan, Z.; Hoatson, G. *Magn. Reson. Chem.* **2002**, *40*, 70.

(24) Yifen, J.; Xiangsheng, C.; Xihuai, H. J. *Non-Cryst. Solids* **1989**, *112*, 147.

(25) Ducel, J. F.; Videau, J. J.; Couzi, M. *Phys. Chem. Glasses* **1993**, *34*, 212.

(26) Hudgens, J. J.; Brow, R. K.; Tallant, D. R.; Martin, S. W. J. *Non-Cryst. Solids* **1998**, *223*, 21.

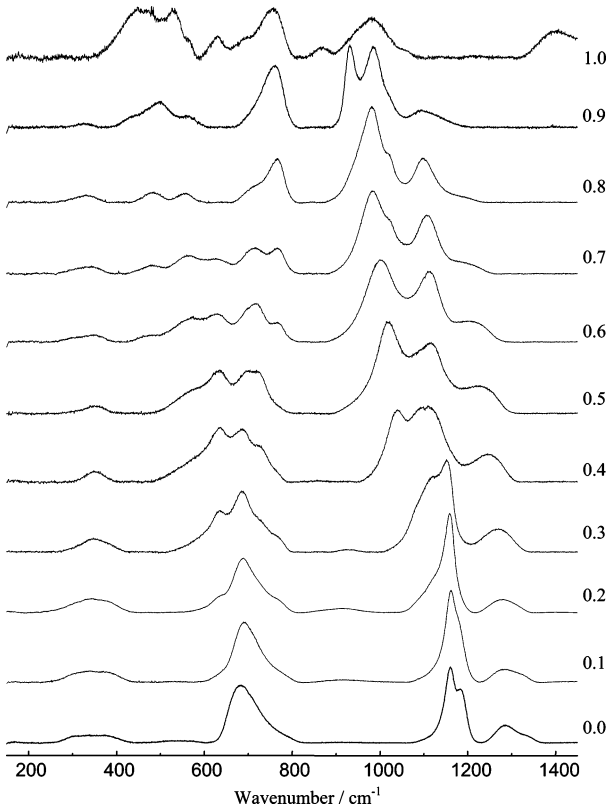

Figure 3. Raman spectra of sodium borophosphate glasses with composition $(Na_2O)_{0.4}[(B_2O_3)_x(P_2O_5)_{1-x}]_{0.6}$ as a function of *x*.

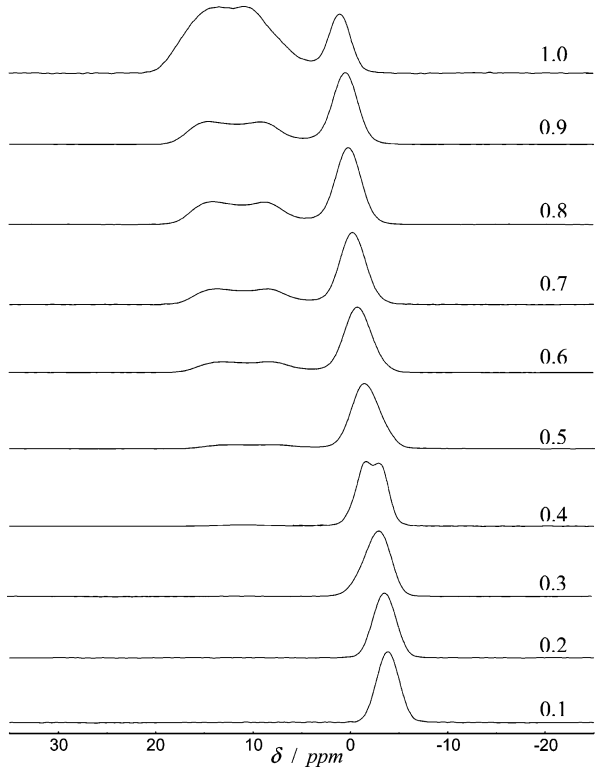

Figure 4. ^{11}B-MAS NMR spectra of sodium borophosphate glasses with composition $(Na_2O)_{0.4}[(B_2O_3)_x(P_2O_5)_{1-x}]_{0.6}$ as a function of *x*.

thermore, the 1161 cm^{-1} band is gradually replaced by a broader signal near 1100 cm^{-1}. Both of these effects, which are most prominently observed in the glasses in the intermediate composition range ($0.7 < x < 0.4$), can be attributed to boron ligation of the $P^{(3)}$ units and the $P^{(2)}$ units, respectively. For glasses with $x > 0.5$, an additional signal near 1000 cm^{-1} is observed, which gradually shifts toward lower wavenumbers as the boron content is increased further. In conjunction with the ^{31}P NMR spectra to be discussed below, we attribute this band to a superposition of signals of the PO_2 vibrations of $P^{(2)}$ units connected to two boron species ($P^{(2)}_{2B}$) and the PO_3 vibrations of $P^{(1)}$ species.[26] Finally, the sharp band seen at 950 cm^{-1} in the $x = 0.9$ sample is assigned to $P^{(0)}$ units. Incorporation of borate produces a new peak at 631 cm^{-1}, which initially increases in intensity with increasing *x* and then diminishes again and shifts to lower wave numbers for higher boron contents ($x > 0.5$). As previously suggested, this line may be attributed to the appearance of $BO_{4/2}^-$ units, abbreviated henceforth $B^{(4)}$.[25] An additional broad feature appearing near 800 cm^{-1} at higher boron contents ($x > 0.5$) signifies boron−oxygen stretching vibrations involving the bridging oxygen atoms that are associated with the $BO_{3/2}$ ($B^{(3)}$) units. The pure sodium borate end-member glass displays a strong band near 1400 cm^{-1}, which can be assigned to B−O stretching vibrations associated with nonbridging oxygen atoms. The noticeable absence of this vibrational mode from the spectra of all the other glasses suggests that the latter do not contain appreciable amounts of nonbridging oxygen species. This conclusion is indeed confirmed by the solid-state NMR data discussed below.

^{11}B MAS NMR. Figure 4 shows the ^{11}B MAS NMR spectra. The ^{11}B spectrum of low-boron-containing glasses consists of a single sharp resonance signifying four-coordinate $B^{(4)}$ units subject to rather weak nuclear electric quadrupolar interactions. For glasses with higher boron contents, a gradual shift toward higher resonance frequencies can be noted, and a two-peak structure becomes apparent at some compositions. For example in the glass with composition $(Na_2O)_{0.4}[(B_2O_3)_{0.4}[P_2O_5)_{0.6})]_{0.6}$, two distinct signals at −1.5 and −3.3 ppm can be resolved. As revealed by previous $^{11}B\{^{31}P\}$ REDOR results on the related silver borophosphate glass system, the site discrimination and the chemical shift trends reflect changes in the extent of B−O−P connectivity as a function of composition.[22] Specifically, the signal at −3.3 ppm can be assigned to $B^{(4)}$ units linked to 3 to 4 P atoms (i.e., $B^{(4)}_{3P}$ and $B^{(4)}_{4P}$ units), whereas the signal near −1.5 ppm is attributed to $B^{(4)}$ units linked to 2 P atoms ($B^{(4)}_{2P}$ units). In addition to the relatively sharp resonance(s) attributed to the $B^{(4)}$ groups, the spectra of glasses with $x > 0.4$ reveal a second signal component having an isotropic chemical shift near 17−18 ppm, which is assigned to three-coordinated $B^{(3)}$ species. The line shape of this component is significantly influenced by second-order quadrupolar perturbation effects, reflecting nuclear electric quadrupolar coupling constant values C_Q near 2.6 MHz. The relative intensity of this signal increases significantly toward higher B_2O_3 contents, and at the highest boron contents near the limit of the glass-formation region, about half of the boron atoms are three-coordinate. A radical change is observed between the sample with $x = 0.9$ and $x = 1.0$, the latter being the pure binary sodium borate glass. In the latter glass, a strong line shape component is found to be characterized

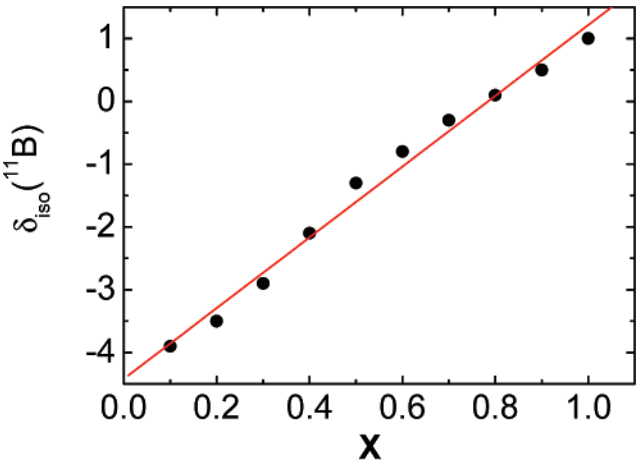

Figure 5. ^{11}B isotropic chemical shift of the $B^{(4)}$ resonance in sodium borophosphate glasses with composition $(Na_2O)_{0.4}[(B_2O_3)_x(P_2O_5)_{1-x}]_{0.6}$. For those glasses in which two resolved $B^{(4)}$ resonances are observed, the weighted average is depicted. The straight line is a linear regression fit to the data.

by a significant asymmetry parameter ($\eta_Q = 0.6$). This signal is assigned to three-coordinate boron atoms bound to one nonbridging oxygen (i.e., $BO_{2/2}O^-$−($B^{(2)}$) units).[27] Analysis of the whole set of spectra reveals that these types of units are present only in binary sodium borate, but not in any of the ternary sodium borophosphate glasses, in agreement with the conclusion from Raman spectroscopy.

Figure 5 reveals that with increasing value of x, the $B^{(4)}$ resonance shifts monotonically toward higher frequencies. As previously noted, this trend reflects a gradual decrease in the average number of B−O−P linkages for these units.[22] On the basis of this correlation, we can estimate the average number of B−O−P linkages, corresponding to the number m in the $B^{(4)}{}_{mP}$ notation, by linear interpolation between the values $\delta_{iso} = 1.0$ ($m = 0$ in the binary borate glass) and $\delta_{iso} = -3.9$ (m is assumed to be close to 4 in the $x = 0.1$ sample). These values are included in Table 2. Finally, on the basis of previous ^{11}B{^{31}P} REDOR results on the analogous silver borophosphate glasses and analogous ones (not reported here) on the present glasses, the $B^{(3)}$ units are assumed to be remote from phosphorus atoms (no B−O−P linkages).

^{31}P MAS NMR. Figure 6 summarizes the ^{31}P MAS NMR results. The spectrum of the pure sodium phosphate glass end-member agrees with that found in the literature.[28] The relative fractions of the $P^{(3)}$ (branching) and $P^{(2)}$ (chain) units are in excellent agreement with the expected 2:1 ratio predicted by the "binary" site modification model. Addition of the borate component leads to the appearance of various distinct new resonances, which can be assigned to $P^{(3)}{}_{mB}$ ($m \leq 3$) and $P^{(2)}{}_{mB}$ ($m \leq 2$) sites arising from the formation of P−O−B linkages. These assignments were recently suggested by ^{31}P{^{11}B} REDOR results on sodium and silver borophosphate glasses of different compositions[21,22] and confirmed by analogous experiments conducted on representative samples of the present glass system (data not shown). Formation of B−O−P links has the effect of

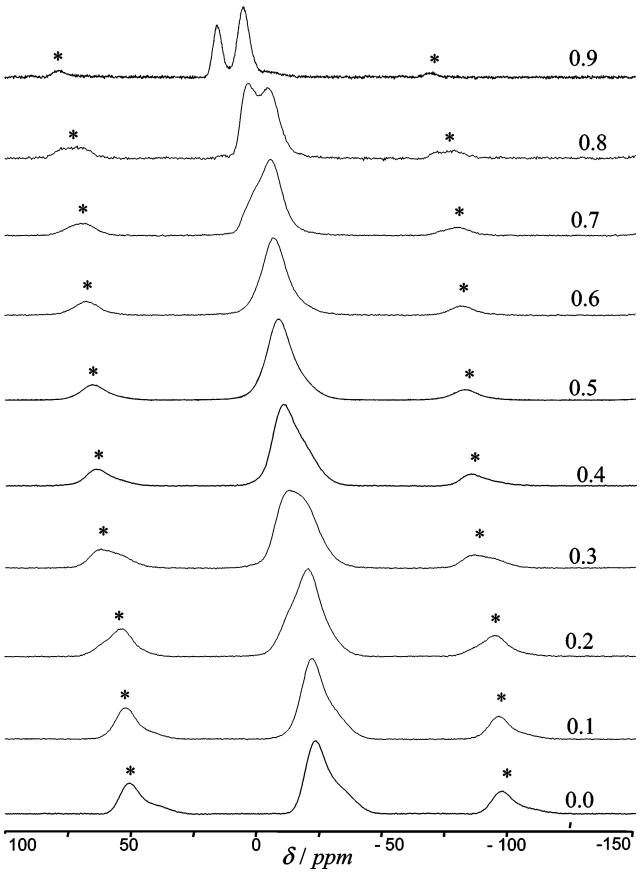

Figure 6. ^{31}P MAS NMR spectra spectra of sodium borophosphate glasses with composition $(Na_2O)_{0.4}[(B_2O_3)_x(P_2O_5)_{1-x}]_{0.6}$ as a function of x. Spinning sidebands are indicated by asterisks.

displacing the resonance of a given $P^{(n)}$ unit toward higher frequencies. The continuous chemical shift trend observed in both of the glass series as a function of composition reveals that, evidently, the number of P−O−B linkages increases with increasing x, although no clear chemical shift discrimination between $P^{(2)}{}_{1B}$ and $P^{(2)}{}_{2B}$ units can be discerned at any of the glass compositions considered. The continuous trend of the signal toward more positive chemical shift values with increasing boron content most likely reflects the changing ratio between $P^{(2)}{}_{1B}$ and $P^{(2)}{}_{2B}$ units; we can quantify this ratio on the basis of the measured chemical shift by interpolating between the extreme values of −12.8 ppm ($P^{(2)}{}_{1B}$ units) and −5.4 ppm ($P^{(2)}{}_{2B}$ units). In addition, resonances attributable to $P^{(3)}{}_{1B}$ and $P^{(3)}{}_{2B}$ units are likely to contribute to the spectra. Finally, at glass compositions with rather high boron contents ($x > 0.7$), the spectra show the formation of $P^{(1)}$ and even $P^{(0)}$ species (peaks near 3 and 10 ppm, respectively). Indeed, this observation is well-correlated with the appearance of the new Raman scattering peaks near 1000 and 950 cm^{-1} (see Figure 3), which are easily assigned to phosphate end groups and isolated PO_4^{3-} units, respectively. Table 3 summarizes the ^{31}P peak deconvolutions into two or three Gauss/Lorentz spectral components and their corresponding assignments.

Discussion

Figure 6 and Table 3 indicate that in the majority of the glasses, the resolution of the ^{31}P MAS NMR spectra is not

(27) Kriz, H. M.; Park, M. J.; Bray, P. J. *Phys. Chem. Glasses* **1971**, *12*, 45.
(28) Brow, R. K.; Kirkpatrick, R. J.; Turner, G. L. J. *Non-Cryst. Solids.* **1990**, *116*, 39.

Table 2. Deconvolution Results of the ^{11}B MAS NMR Spectra of Sodium Borophosphate Glasses with Compositions $(Na_2O)_{0.4}[(B_2O_3)_x[P_2O_5)_{1-x})]_{0.6}$

x	position δ_{iso} (± 0.1 ppm)	fwhm $\Delta\nu$ (± 0.2 ppm)	G/L	C_Q (± 0.05 MHz)	η_Q	area (± 2%)	structural groups
0.1	−3.9	2.7	0.97			100.0	$B^{(4)}_{mP}$ $m = 4.0$
0.2	−3.5	2.7	0.93			100.0	$B^{(4)}_{mP}$ $m = 3.67$
0.3	−1.0	1.7	0.06			13.2	$B^{(4)}_{mP}$ $m = 1.63$
	−3.2	2.9	0.91			86.8	$B^{(4)}_{mP}$ $m = 3.43$
0.4	−1.5	2.2	0.73			61.3	$B^{(4)}_{mP}$ $m = 2.04$
	−3.3	1.8	0.90			35.9	$B^{(4)}_{mP}$ $m = 3.51$
	n.d.			n.d.	n.d.	2.7	$B^{(3)}$
0.5	−1.1	2.9	1.0			59.3	$B^{(4)}_{mP}$ $m = 1.71$
	−2.7	3.0	1.0			25.0	$B^{(4)}_{mP}$ $m = 3.02$
	16.3	3.1	-	2.52	0.28	15.7	$B^{(3)}$
0.6	−0.8	3.3	0.89			66.3	$B^{(4)}_{mP}$ $m = 1.47$
	17.1	3.1	-	2.59	0.31	33.7	$B^{(3)}$
0.7	−0.3	3.1	0.86			58.8	$B^{(4)}_{mP}$ $m = 1.06$
	17.6	3.1	-	2.61	0.28	41.2	$B^{(3)}$
0.8	0.1	3.0	0.88			51.1	$B^{(4)}_{mP}$ $m = 0.74$
	17.9	3.1	-	2.61	0.28	48.9	$B^{(3)}$
0.9	0.5	2.9	0.87			48.2	$B^{(4)}_{mP}$ $m = 0.41$
	18.3	3.1	-	2.61	0.28	51.8	$B^{(3)}$
1.0	18.8	3.1	-	2.49	0.60	43.8	$B^{(2)}$
	18.6	3.1	-	2.60	0.20	39.0	$B^{(3)}$
	1.0	2.5	0.97			17.2	$B^{(4)}$ $m = 0.0$

Table 3. Deconvolution Results of the ^{31}P MAS NMR Spectra of Sodium Borophosphate Phosphate Glasses with Compositions $(Na_2O)_{0.4}[(B_2O_3)_x[P_2O_5)_{1-x})]_{0.6}$

x	position δ_{iso} (± 0.1 ppm)	fwhm $\Delta\nu$ (± 0.2 ppm)	G/L	area (± 2%)	structural groups
0	−22.7	8.8	0.94	64.7	$P^{(2)}$
	−32.3	12.7	1.00	35.3	$P^{(3)}$
0.1	−17.2	9.1	0.54	4.8	$P^{(2)}_{1B}$
	−21.4	8.9	0.81	62.3	$P^{(2)} + P^{(3)}_{2B}$
	−29.9	12.9	0.90	32.9	$P^{(3)} + P^{(3)}_{1B}$
0.2	−12.8	9.5	1.0	25.5	$P^{(2)}_{1B}$
	−20.3	9.1	1.0	53.5	$P^{(2)} + P^{(3)}_{2B}$
	−26.5	12.7	1.0	21.0	$P^{(3)} + P^{(3)}_{1B}$
0.3	−10.4	9.5	0.46	43.7	$P^{(2)}_{1B} + P^{(2)}_{2B}$
	−16.8	10.9	0.99	30.6	$P^{(2)}_{1B} + P^{(3)}_{2B}$
	−22.6	12.0	0.76	25.7	$P^{(3)}_{1B} + P^{(2)}$
0.4	−9.2	8.6	0.82	43.1	$P^{(2)}_{1B} + P^{(2)}_{2B}$
	−15.5	13.1	0.55	52.8	$P^{(3)}_{2B} + P^{(2)}_{1B}$
	−22.2	8.2	1.0	4.1	$P^{(3)}_{1B}$
0.5	−8.5	11.4	0.66	85.6	$P^{(3)}_{3B} + P^{(2)}_{2B}$
	−19.2	8.7	0.15	14.4	$P^{(3)}_{2B}$
0.6	−5.9	11.0	0.81	96.2	$P^{(3)}_{3B} + P^{(2)}_{2B}$
	−17.2	8.7	1.0	3.8	$P^{(3)}_{2B}$
0.7	2.4	7.0	1.0	12.2	$P^{(1)}_{1B}$
	−5.4	10.3	0.46	87.8	$P^{(3)}_{3B} + P^{(2)}_{2B}$
0.8	14.4	4.1	1.0	0.8	$P^{(0)}$
	3.9	6.1	1.0	31.5	$P^{(1)}_{1B}$
	−4.2	10.3	0.7	68.7	$P^{(2)}_{2B}$
0.9	15.6	4.1	0.98	27.9	$P^{(0)}$
	5.3	5.4	0.52	64.3	$P^{(1)}_{1B}$
	−5.4	11.1	0.04	7.8	$P^{(2)}_{2B}$

complete. At most, three distinct spectral components can be identified, each of which still represents a superposition of signals arising from different species. For example, in the $x = 0.2$ sample, the peak observed near −20.3 ppm most likely comprises the signals of both $P^{(2)}$ and $P^{(3)}_{2B}$ units. Still, we can estimate the individual contributions of both species to this signal by considering the fact that the total number of anionic charges in the glass must equal the total number of sodium ions present. Taking into consideration that at this particular glass composition all the boron species are anionic $B^{(4)}$groups ($N_4 = 1$), we can conclude that the −20.3 ppm peak in this particular sample is comprised of roughly comparable contributions from anionic $P^{(2)}$ and neutral $P^{(3)}_{2B}$ units. This calculation goes as follows: The $x = 0.2$ sample contains 40 mol % Na_2O, 48 mol % P_2O_5, and 12 mol % B_2O_3. Because according to the ^{11}B NMR data, all of the boron species are anionic, 12 mol % Na_2O is consumed for the modification of the boron species in the network, leaving 28 mol % Na_2O for the modification of the phosphorus species. Thus, of the 48 mol % P_2O_5 present in the sample, 28 mol % is present as anionic $P^{(2)}$ units (corresponding to 28/48 = 58% of the total phosphorus present), and 20 mol % must be present as neutral $P^{(3)}$ units (corresponding to 20/48 = 42% of the total phosphorus present). According to Table 3, the ^{31}P NMR spectrum can be deconvoluted into three signal components with the area ratios listed there. On the basis of its chemical shift, the component at −12.8 ppm, which corresponds to 25.5% of the total area in the ^{31}P spectrum, is assigned to a $P^{(2)}_{1B}$ unit. Furthermore, the component at −26.5 ppm, which corresponds to 21% of the total area, is assigned to neutral $P^{(3)}_{1B}$ and $P^{(3)}_{0B}$ units. Now, the central resonance at −20.3 ppm, which contains 53.5%

Table 4. Relative Speciations (Percent (± 2%) of the Phosphorus and Boron Species, Respectively) in Sodium Borophosphate Glasses Calculated According to the Charge Compensation Rules and on the Basis of the Isotropic Chemical Shift Assignments of Various Phosphate and Borate Units

	amount in %										
	0.0	0.1	0.2	0.3	0.4	0.5	0.6	0.7	0.8	0.9	1.0
$P^{(0)}$									1	28	
$P^{(1)}_{1B}$								9	32	64	
$P^{(2)}_{0}$	65	~58	~33	~2							
$P^{(2)}_{1B}$		5	25	34	24	20	3				
$P^{(2)}_{2B}$				17	22	29	64	67	69	8	
$P^{(3)}_{0}$	35	~2									
$P^{(3)}_{1B}$		~31	21	~23	4						
$P^{(3)}_{2B}$		~4	~21	~24	50	51	33				
$P^{(3)}_{3B}$								24			
$B^{(2)}_{2B}$											44
$B^{(3)}_{nB}$					3	16	34	42	49	52	39
$B^{(4)}_{nB}$				13	61	59	66	58	51	48	17
$B^{(4)}_{4P} + B^{(4)}_{3P}$		100	100	87	36	25					

of the total signal area, contains overlapping contributions from both anionic $P^{(2)}{}_{0B}$ (percentage x) and $P^{(3)}{}_{2B}$ units (percentage $53.5 - x$). Because the total $P^{(2)}/P^{(3)}$ ratio must be 58:42 in this sample, we have the condition $58 = 25.5 + x$ (and analogously $42 = 21 + (53.5 - x)$), resulting in $x = 32.5\%$ (rounded to 33% in Table 4). On the basis of analogous considerations, the relative boron and phosphorus speciations, expressed as percentages of the total boron and phosphorus contents, respectively, have been extracted from the spectra and are listed in Table 4. By multiplying these percentages with the actual boron and phosphorus concentrations present in these glasses, we arrive at the absolute boron and phosphorus species concentrations, which are plotted in Figure 7. For each glass composition, the individual entries in this Figure sum up to 60 mol %, corresponding to the total network former concentration.

Clearly, the structural transformation of sodium borophosphate units can be divided into three compositional regions. Within the phosphate-rich domain I ($0 \le x \le 0.4$), the most dramatic change is the rapid increase in the number of $B^{(4)}$ units, accompanied by the diminution of the metaphosphate-type chain units. In this region, the concentration of the $P^{(3)}$ units increases with increasing x, because the boron constituent consumes more sodium for modification than predicted from the network former to network modifier ratio (0.67) present in the glass. Within domain I, this redistribution of the network modifier results in an increase of the average degree of polymerization of the phosphate species, even though the Na/P ratio increases. Although in pure binary alkali phosphate glasses the $P^{(3)}$ units are known to be rather unstable, the evidence presented here suggests that they can be significantly stabilized by the formation of P−O−B linkages. We note that the behavior observed here is in striking contrast to the binary sodium phosphate system, in which the degree of condensation decreases continually as the Na/P ratio increases.

For intermediate compositions (domain II, $0.4 \le x \le 0.8$), both the concentrations of the $P^{(2)}$ and the $B^{(4)}$ units remain approximately constant. In this region, the main structural change is the decrease of the concentration of the $P^{(3)}$ groups, concurrent with the increase in the concentrations of the $B^{(3)}$

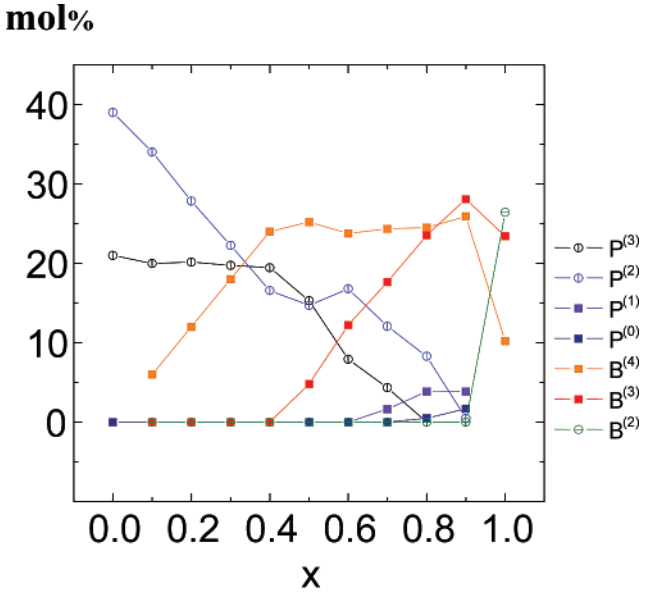

Figure 7. Absolute concentrations (in mol %) of individual phosphorus and boron environments in sodium borophosphate glasses with composition $(Na_2O)_{0.4}[(B_2O_3)_x(P_2O_5)_{1-x}]_{0.6}$. For each composition, the individual entries sum to 60 mol %, corresponding to the constant network former content present in these glasses.

units. At even higher borate contents (domain III: $x = 0.8$, 0.9), the concentration of the $P^{(2)}$ units decreases further (they are replaced by $P^{(1)}$ and $P^{(0)}$ units), the concentration of $B^{(4)}$ still remains constant, whereas the contribution of $B^{(3)}$ to the network keeps increasing. In this region, the formation of doubly and triply charged phosphate species along with the observation of large amounts of neutral $B^{(3)}$ groups clearly indicates a net charge transfer occurring from the borate to the phosphate network. This particular property by which the phosphorus atoms compete successfully against the other network formers for the additional network modifier oxide has been reported for other borophosphate glasses.[22] Finally, in the pure sodium borate glass end-member, the situation is entirely different. The amount of $B^{(4)}$ units is drastically decreased and a new anionic three-coordinate type of boron unit $B^{(2)}$ appears that bears two bridging and one nonbridging oxygen atoms. These $B^{(2)}$ units are not found in any of the ternary glasses. The dramatic change in going from the ternary to the binary glass system indicates that the tetrahedral $B^{(4)}$ units observed in the borate-rich domain must be stabilized by the formation of B−O−P linkages. Indeed, the existence of these links has been previously established by $^{11}B\{^{31}P\}$ REDOR data obtained on analogous silver borophosphate glasses.[22]

From the detailed structural analysis reported above, we can determine the average number of bridging oxygen species per network former, [O], which corresponds to the overall degree of network polymerization. Considering the fact that each bridging oxygen species makes one link between two network former species, [O] has values of 0.5, 1.0, and 1.5 for the $P^{(1)}$, $P^{(2)}$, and $P^{(3)}$ species, and 1, 1.5. and 2.0 for the $B^{(2)}$, $B^{(3)}$, and $B^{(4)}$ units, respectively. As shown in Figure 8, [O] increases significantly in domain I (reflecting the structural changes discussed above) and remains approximately constant in domains II and III. Finally, [O] is dramatically decreased in the binary sodium borate end-

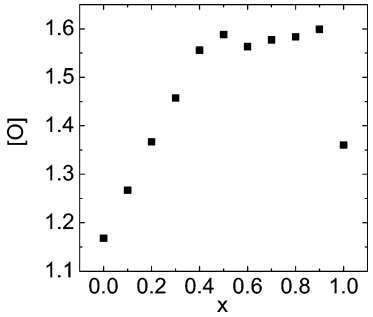

Figure 8. Number of bridging oxygen species per network former unit in sodium borophosphate glasses with composition $(Na_2O)_{0.4}[(B_2O_3)_x(P_2O_5)_{1-x}]_{0.6}$.

Table 5. Composition Dependence of the Numbers of the Various Types of Bridging Oxygen Species Per Network Former Unit (±0.02)

x	[**P**−O−P]	[**P**−O−B]	[**B**−O−B]	[**O**]
0	1.18	0	0	1.18
0.1	0.87	0.40	0	1.27
0.2	0.62	0.72	0.04	1.37
0.3	0.33	0.96	0.12	1.46
0.4	0.25	1.02	0.28	1.54
0.5	0.18	0.89	0.52	1.59
0.6	0.07	0.68	0.82	1.56
0.7	0	0.54	1.04	1.58
0.8	0	0.32	1.25	1.57
0.9	0	0.13	1.48	1.61
1.0	0	0	1.37	1.37

member of this glass series, because of the different nature of the dominant anionic boron species in this glass. The comparison with the binary glasses sodium borate and sodium phosphate clearly demonstrates that the combined presence of the network formers P_2O_5 and B_2O_3 results in a significant enhancement of network polymerization, manifesting a "mixed network-former effect". In this connection, the striking resemblance of the plots [O](x) (Figure 8) and T_g(x) (Figure 1) clearly suggests that the compositional trend of the glass-transition temperature in this system can be explained on the basis of the average network connectivity concept. Even more interesting, exactly analogous compositional dependences can be observed for the ionic conductivity and its corresponding activation energy. More specifically, comparison of Figures 2 and 6 indicates that electrical conductivity and absolute concentration of $B^{(4)}$ units show nearly the same dependence on the compositional parameter x. This result, in turn, suggests that the concentration of these $B^{(4)}$ units may be a critical structural parameter influencing the mobility of the ions. According to these results, the anionic $BO_{4/2}$ units may represent binding sites that are particularly conducive to ionic motion, at least in comparison to their anionic alternatives, i.e., the $P^{(2)}$ and $B^{(2)}$ groups.

Finally, the number of bridging oxygen species per network former species, [O], is made from the individual contributions of P−O−P, P−O−B, and B−O−B linkages. We can extract approximate numbers for these three contributions from the ^{31}P and ^{11}B MAS NMR peak deconvolutions (see Table 5 and Figure 9). As a matter of fact, two independent values for [P−O−B] can be extracted from either the ^{31}P or the ^{11}B MAS NMR spectra. The fact that these respective values are well consistent with each other (see Figure 10) justifies the assumptions made in arriving at the analysis described above. Specifically, the result validates

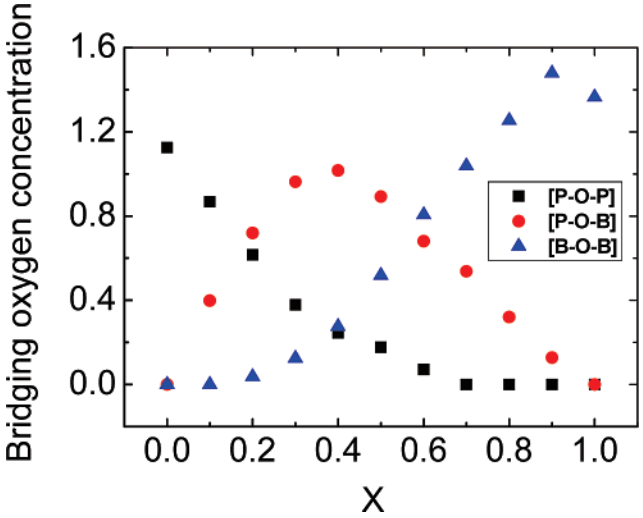

Figure 9. Number of the various types of bridging oxygen species per network former unit as a function of composition. Symbol sizes represent experimental error estimates.

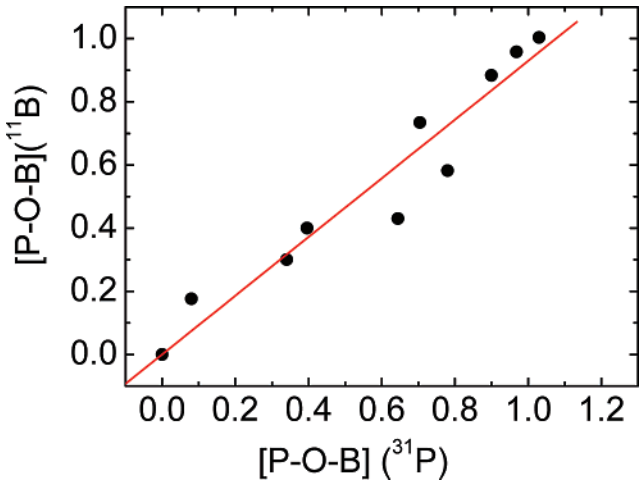

Figure 10. Number of [P−O−B] linkages per network former species determined from ^{11}B versus the corresponding number deduced from ^{31}P MAS NMR. Symbol sizes represent experimental error estimates.

the quantitative analysis of the overlapped ^{31}P spectra, the chemical shift analysis of the $^{11}B^{(4)}_{mP}$ resonance in terms of the average number of connected P atoms, and the assumption that the three-coordinate boron species are not linked to P atoms. Figure 9 documents the strongly favorable interaction between the borate and the phosphate units in the network, producing a number of B−O−P linkages that is close to the maximum value possible at any given composition, as previously suggested on the basis of qualitative ^{17}O NMR data.[21] For future studies, it would be of interest to compare the predicted concentrations of oxygen species predicted from the present work to corresponding values extracted from quantitative ^{17}O MQMAS-NMR spectroscopic data.

Conclusions

In summary, a detailed structural analysis of sodium borophosphate glasses within the composition range $(Na_2O)_{0.4}[(B_2O_3)_x(P_2O_5)_{1-x}]_{0.6}$ with $0.0 \leq x \leq 1.0$ has been presented on the basis of the detailed quantitative analysis of ^{11}B and ^{31}P MAS NMR spectra. These data illustrate

unambiguously the preferential formation of B−O−P linkages between $P^{(3)}$ branching units and tetrahedral boron species. A particular consequence of this favorable interaction is an increase in the degree of network polymerization as quantified by the number of bridging oxygen species per network former. On this basis, we can rationalize the enhanced glass-transition temperatures of the ternary glasses in comparison to the binary glass end members.

The strong correlation of T_g with the degree of average network polymerization deserves some further comment, however. Although for covalent (chalcogenide) glasses, the concept of average coordination number has been applied very successfully for explaining the compositional evolution of their physical properties,[29] its applicability to oxide glasses has been much more limited. For example, in the $(Na_2O)_x$-$(SiO_2)_{1-x}$ glass system, T_g tends to decrease with increasing x,[30] whereas in the $(Na_2O)_x$-$(P_2O_5)_{1-x}$ glass system, a rather complex dependence on x is observed, showing an increase of T_g with x for $x > 0.2$.[31] Thus opposite trends are observed even though in both glass systems an increase in the network modifier content x decreases the degree of network polymerization. This striking difference illustrates that the physical properties of oxide glasses are also influenced by effects other than framework connectivity, for example, Coulomb and dipolar forces. In the present glass system, these additional contributions do not change much as a function of composition (the cation concentrations are kept approximately constant), thereby allowing us to expose the significance of the average network connectivity for macroscopic properties in oxide glasses.

Acknowledgment. Funding by the Deutsche Forschungsgemeinschaft, SFB 458, is most gratefully acknowledged. D.Z. thanks the NRW Graduate School of Chemistry for a personal stipend. We also thank Ms. Wilma Pröbsting for the thermoanalytical characterization.

CM0628092

(29) Tatsumisago, M.; Halfpap, B. L.; Green, J. L.; Lindsay, S. M.; Angell, C. A. *Phys. Rev. Lett.* **1990**, *64*, 1549.
(30) Scholze, H. *Glass—Nature, Structure and Properties*; Springer-Verlag: Berlin, 1988.
(31) Hudgens, J. J.; Martin, S. W. *J. Am. Ceram. Soc.* **1993**, *76*, 1691.